

Research Article

The Effect of Transition Metal Doping on the Photooxidation Process of Titania-Clay Composites

Judit Ménesi,¹ Renáta Kékesi,¹ László Körösi,¹ Volker Zöllmer,² André Richardt,³ and Imre Dékány¹

¹ Department of Colloid Chemistry, Supramolecular and Nanostructured Materials Research Group of Hungarian Academy of Sciences, University of Szeged, H-6720 Szeged, Aradi Vertanuk tere 1, Hungary

² Fraunhofer Institute for Manufacturing and Advanced Materials (IFAM), Functional Structures, Wiener Strasse 12, 28359 Bremen, Germany

³ German Armed Forces Scientific Institute for Protection Technologies, NBC-Protection, 29623 Munster, Germany

Correspondence should be addressed to Imre Dékány, i.dekany@chem.u-szeged.hu

Received 8 September 2007; Accepted 23 November 2007

Recommended by M. Sabry A. Abdel-Mottaleb

Montmorillonite-TiO₂ composites containing various transition metal ions (silver, copper, or nickel) were prepared, and their photocatalytic efficiencies were tested in the degradation of ethanol vapor at 70% relative humidity. Two light sources, UV-rich ($\lambda = 254$ nm) and visible ($\lambda = 435$ nm), were used. The kinetics of degradation was monitored by gas chromatography. It was established that, in the case of each catalyst, ethanol degradation was more efficient in UV-C ($\lambda = 254$ nm) than in visible light, furthermore, these samples containing silver or copper ions were in each case about twice more efficient than P25 TiO₂ (Degussa AG.) used as a reference. In photooxidation by visible light, TiO₂/clay samples doped with silver or copper were also more efficient than the reference sample, P25 TiO₂. We show that doping metal ions can also be delivered to the surface of the support by ion exchange and significantly alters the optical characteristics of the TiO₂/clay composite.

Copyright © 2008 Judit Ménesi et al. This is an open access article distributed under the Creative Commons Attribution License, which permits unrestricted use, distribution, and reproduction in any medium, provided the original work is properly cited.

1. INTRODUCTION

The photocatalytic degradation of volatile organic compounds (VOCs) by UV light in the presence of TiO₂ catalysts has been the subject of numerous publications [1–10]. TiO₂ is one of the most efficient photocatalysts; however, since semiconductor particles are in need of the higher energy content of UV light, a mere 5% of sunlight is utilized in the course of irradiation for excitation of the catalyst. Absorption by photocatalysts in the visible range can be significantly improved by incorporation of metal ions; however, photoactivity is highly dependent on the chemical nature and the concentration of the doping ion and on the method of preparation. Dvoranová et al. [11] incorporated cobalt, chrome, and manganese ions into the crystalline structure of TiO₂ using the sol-gel method. Although the presence of the doping ions caused a significant absorption shift in the visible range relative to pure P25 titanium dioxide, the photocatalytic activity of the catalysts decreased considerably. Chiang et al. [12] prepared Degussa P25 TiO₂ doped with CuO by photodeposition for the purpose of liquid-phase degradations;

the presence of Cu²⁺ ions, however, again decreased photocatalytic efficiency. TiO₂ doped with CuO was also prepared by Slamet et al. [13], and enhanced photocatalytic effect was observed only at a single optimal Cu(II) ion content. Copper is an efficient electron trap and is therefore capable of inhibiting recombination of electron-hole pairs, thereby significantly increasing efficiency.

It has been proven by many reports that the reaction rate is dependent on how the component to be destroyed can be concentrated on the surface of TiO₂ [14, 15]. TiO₂-pillared clay minerals, these novel photocatalysts, attract attention by their ability to accelerate the photocatalytic reaction by their unique adsorption capabilities [16, 17]. This increased absorbability is the result of the large specific surface area produced by the incorporation of TiO₂ particles among the silicate layers, creating a mesoporous structure. Liu et al. [18] obtained an Ag-TiO₂/montmorillonite composite by hydrolysis of TiCl₄ and, due to the large specific surface area and the effect of silver content to improve light absorption, they observed an increased photooxidation activity as compared to the reference material, TiO₂. Kun et al. [19] established that

TiO₂/montmorillonite nanocomposites pillared with TiO₂ nanoparticles exhibit outstanding catalytic activity in phenol degradation.

Volatile organic components are being widely utilized not only for industrial but also for household purposes, leading to water and air pollution. Photocatalytic degradation of ethanol has been discussed in detail in a number of studies [20–22]. Nimlos et al. [23] studied the mechanism of degradation and established the following sequence of products: ethanol → acetaldehyde → acetic acid → formaldehyde → formic acid → CO₂, with acetaldehyde as the main intermediate. Sauer and Ollis studied deactivation of Degussa P25 TiO₂ [24, 25]. In the presence of water vapor, intermediates and/or products may accumulate on the surface of the catalyst and deactivate it. Since water is one of the products of the reaction, the reaction rate decreases continuously due to deactivation.

Our objective was the production of catalysts also efficient in the visible range. As shown by the references above, incorporation of metal ions into TiO₂ is not always expedient; we therefore prepared composites with the transition metal ions incorporated not directly on the surface or into the crystalline structure of TiO₂, but into the clay mineral acting as support. When the photocatalyst TiO₂ is mixed to or ground with the clay mineral support, the result is a TiO₂/layer silicate composite held together by electrostatic forces [19]. We study the catalytic properties of the ion-exchanged composite, obtained in this way in ethanol degradation on the solid/gaseous interface at 70% relative humidity, to appropriately model local environmental conditions in the photocatalytic reaction.

2. EXPERIMENTAL

2.1. Materials

Starting materials for the preparation of composites were Degussa P25 TiO₂ and the fine fraction of Na-montmorillonite EXM-838 ($d < 2$ nm, Süd-Chemie AG, Munich, Germany). The following nitrates were used for ion exchange in clay minerals: nickel nitrate (Fluka Chemie GmbH, Buchs, Switzerland), copper nitrate (LightTech, Dunakeszi, Hungary), and silver nitrate (LightTech, Dunakeszi, Hungary). Vapor phase degradation was performed using 99.8% anhydrous ethanol (LightTech, Dunakeszi, Hungary).

2.2. Preparation of transition metal exchanged montmorillonite/TiO₂ composites

One gram of Na-montmorillonite (EXM838) was left to swell in 100 mL of distilled water for 1 day. The next day, 1 mmol of Ag(I) nitrate or 0.5 mmol of Ni(II) and Cu(II) nitrate were added to the montmorillonite swollen in distilled water, the volume of the medium was brought up to 500 mL by the addition of distilled water, and the suspension was left to stand in a hot air thermostat at 35°C for 2 days. The precipitate obtained was next washed 3 times in distilled water, centrifuged and dried at 65°C. The composite was prepared by grinding, for 30 minutes in an agate mortar, a powder mixture consist-

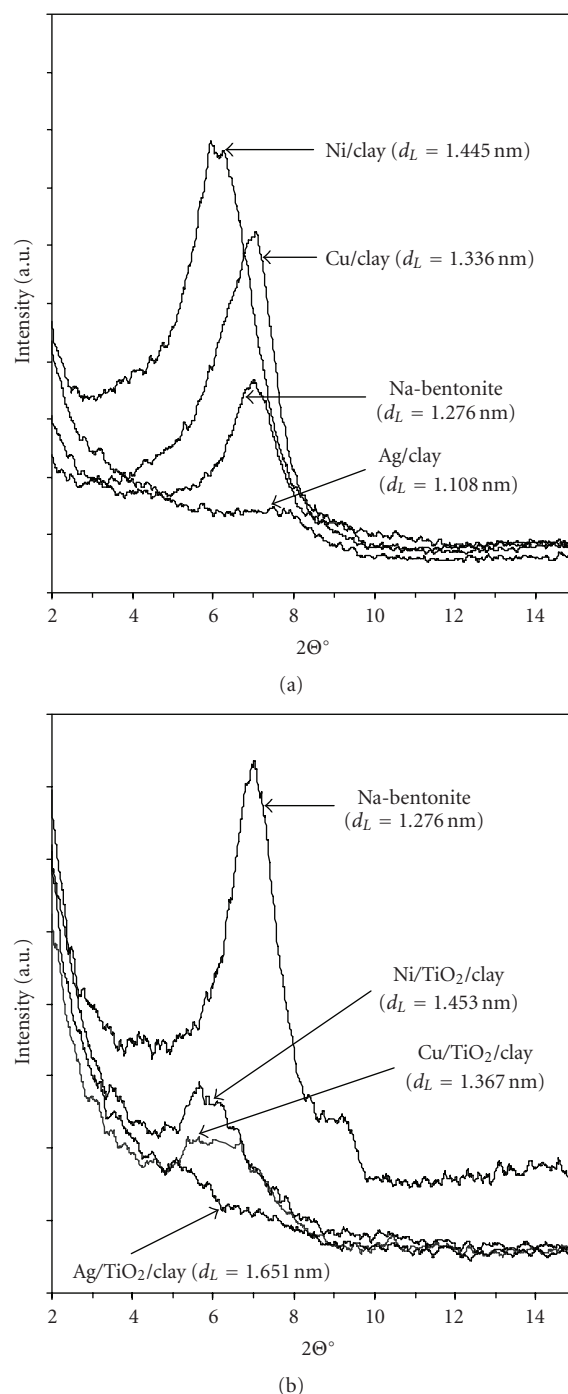


FIGURE 1: X-ray diffraction (XRD) patterns of (a) Me/clay and (b) Me/TiO₂/clay samples.

ing of 20% exchanged transition metal-montmorillonite and 80% P25 TiO₂. Metal contents relative to the total mass of the catalyst were Ag: 2.16%, Cu: 0.64%, and Ni: 0.59%.

2.3. Structure properties

The XRD experiments (Figure 1) were carried out in a Philips X-ray diffractometer (PW 1830 generator, PW 1820

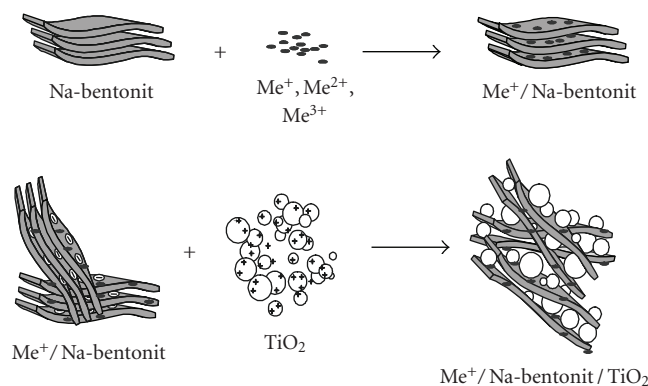
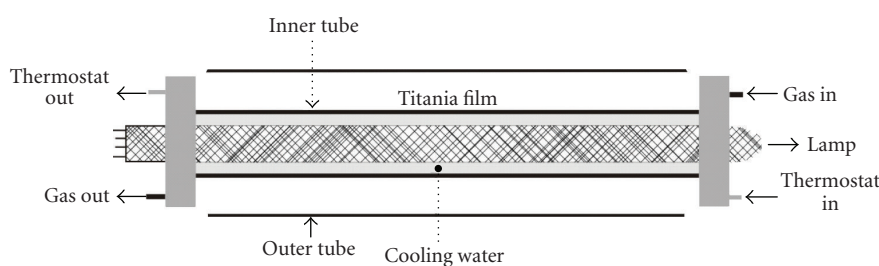
FIGURE 2: Schematic drawing of preparation of Me-ion exchanged montmorillonite/ TiO_2 composites.

FIGURE 3: Schematic drawing of the photoreactor.

goniometer) with $\text{CuK-}\alpha$ radiation ($\lambda = 0.1542 \text{ nm}$) 40 kV, 35 mA. The basal spacing (d_L) was calculated from the (001) reflection via the Bragg equation using the PW 1877 automated powder diffraction software. The analyses were carried out at ambient temperature in the $1\text{--}15^\circ$ (2Θ) ranges. The $1\text{--}15^\circ$ (2Θ) ranges are characteristic of the structure of the layer silicate.

2.4. Optical properties

A Mikropack Nanocalc 2000 spectrophotometer equipped with an integrated sphere (ISP-50-8-R-GT) was used to record the diffuse reflectance spectra of the samples. The spectra of the samples were analyzed under ambient condition in the wavelength range of 350–700 nm. The optical properties of transition metal-loaded titania/clay catalysts are listed in Table 1.

2.5. Photocatalytic reactions

Photooxidation of ethanol was performed in the reactor (volume: ca. 700 mL) at $25 \pm 0.1^\circ\text{C}$. The experimental setup is described in our previous paper [26]. The photoreactor (Figure 3) consists of two concentrically positioned tubes, namely, an inner quartz tube and an outer Pyrex glass tube. The light sources of the reactor were two types of 15 W low-pressure mercury lamp (LightTech, Dunakeszi, Hungary), namely, a GCL307T5L/CELL type (light source 1) with characteristic emission wavelength at $\lambda_{\text{max}} = 254 \text{ nm}$ and a GCL303T5 S#2 type (light source 2) with characteristic emission wavelength at $\lambda_{\text{max}} = 435 \text{ nm}$. The catalyst was sprayed

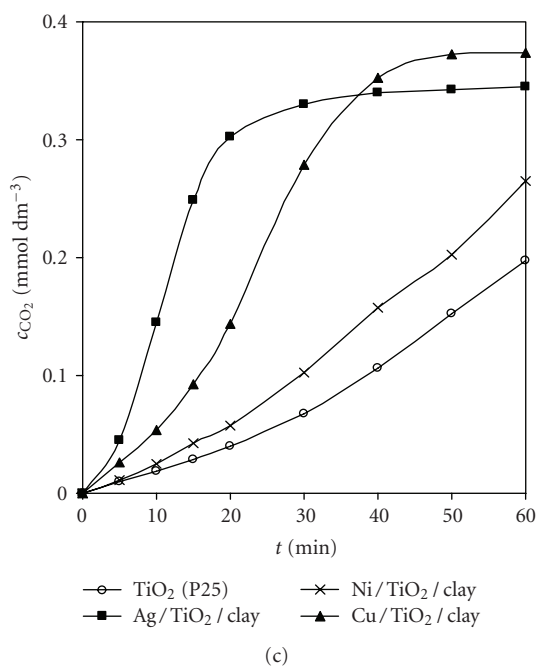
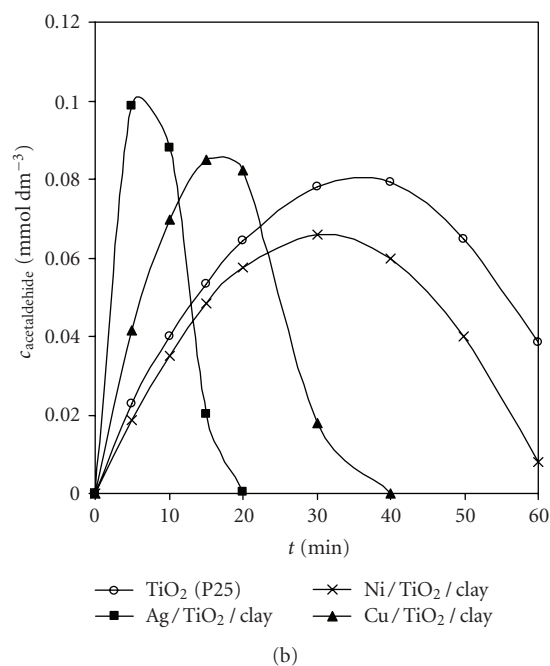
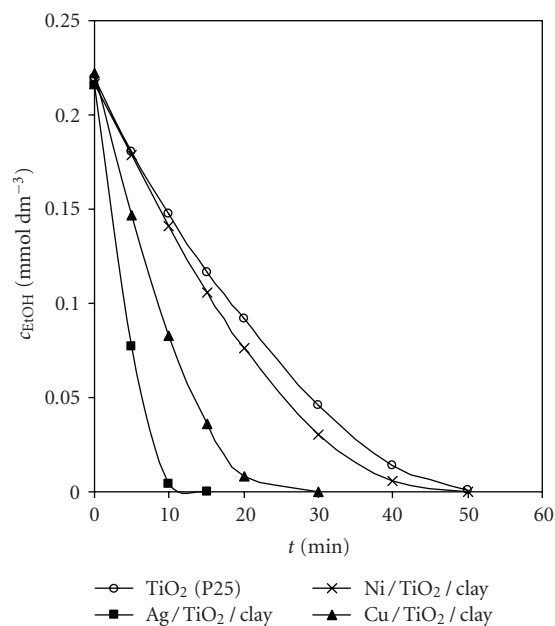
onto the outer side of the inner quartz tube from 10 to 20 (m/v)% aqueous dispersion using N_2 stream. The surface of the catalyst film was 44.8 cm^2 , and the catalyst mass per unit surface was $0.310 \pm 0.03 \text{ mg/cm}^2$. The film thickness was ca. $0.7\text{--}1.0 \mu\text{m}$. The reactor was filled with dry synthetic air ($[\text{H}_2\text{O}] < 5 \text{ ppm}$) to a final pressure of 760 Torr. After the delivery of $10 \mu\text{L}$ ethanol and $12 \mu\text{L}$ water, the system was left to stand for 30 minutes for evaporation of the components and establishment of the adsorption equilibrium. The reaction starts with switching on the lamp. Sampling from the gas phase (1 mL) was performed at selected time intervals, and the composition was analyzed in a gas chromatograph (Shimadzu GC-14B) equipped with a thermal conductivity (TCD) and a flame ionization detector (FID). The temperature of the column (HayeSep Q, length 2 m) was 140°C . A sample volume of 1 mL was introduced through a six-way valve to the online GC used for quantitative analysis of ethanol, acetaldehyde, and CO_2 . A membrane pump inserted into the experimental assembly circulates the gas mixture to be degraded through the flow meter, the reactor, and the sampler of the gas chromatograph. The flow rate of the gas mixture in the measuring system was 375 mL/min . The initial concentration of ethanol was $0.25 \text{ mmol dm}^{-3}$ at relative humidity of $\sim 70\%$.

3. RESULTS

Showing the XRD pattern, we can establish that for the sodium montmorillonite, characteristic Bragg peak at $2\Theta^\circ = 7.02^\circ$ appears and the basal distance is $d_{001} = 1.276 \text{ nm}$. After

TABLE 1: The composition and optical properties of the catalysts.

	Metal content (mequ/g clay)	Metal content (wt%)	λ_g (nm)	E_g (eV)
TiO ₂ (P25)	0.00	0.00	390	3.18
Ag/TiO ₂ /clay	1.00	2.16	455	2.73
Ni/TiO ₂ /clay	1.00	0.59	404	3.07
Cu/TiO ₂ /clay	1.00	0.64	409	3.03

FIGURE 4: Ethanol concentration changes under (a) UV-Vis irradiation (light source 1), (b) kinetic curves of acetaldehyde, and (c) CO₂ formation.

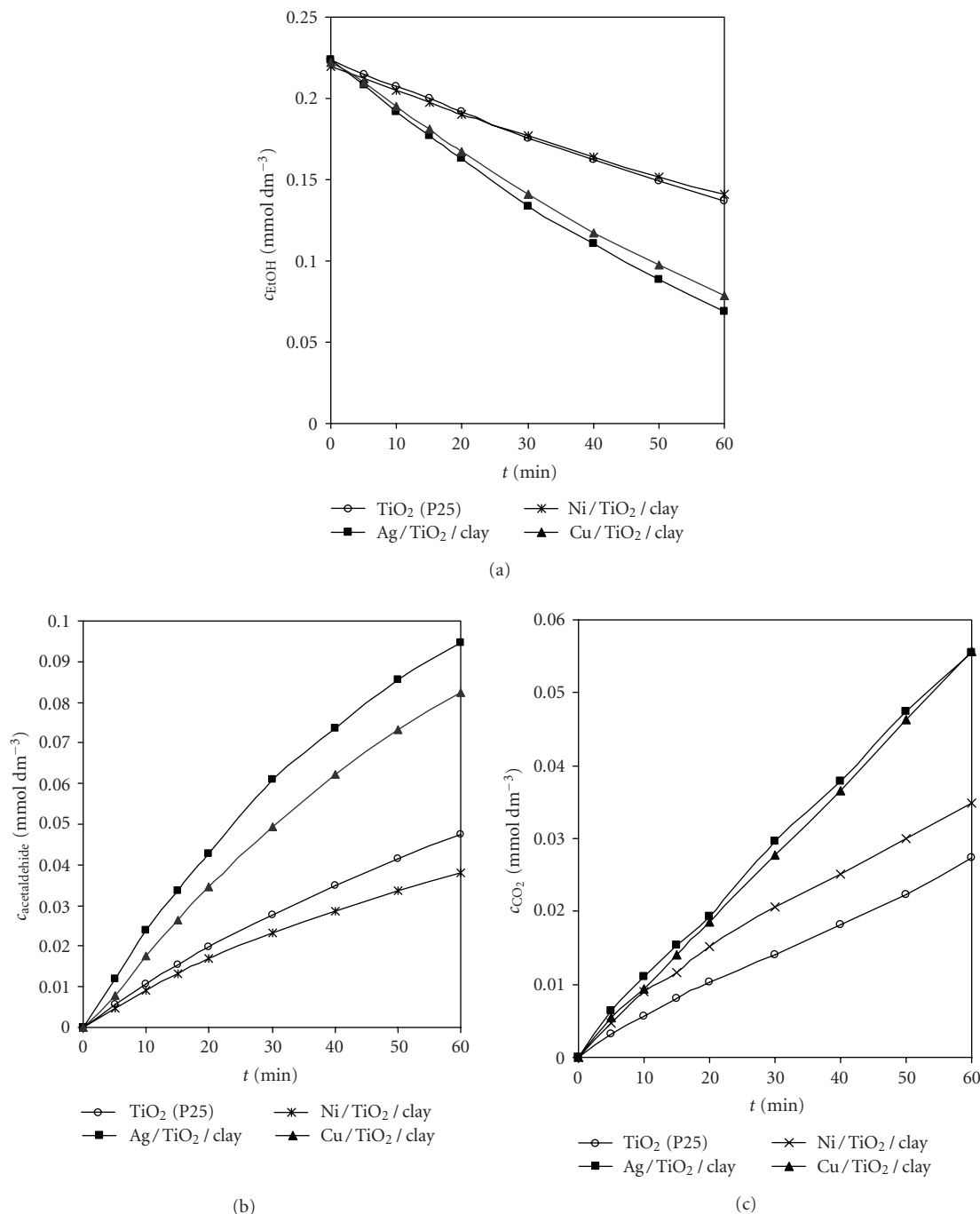


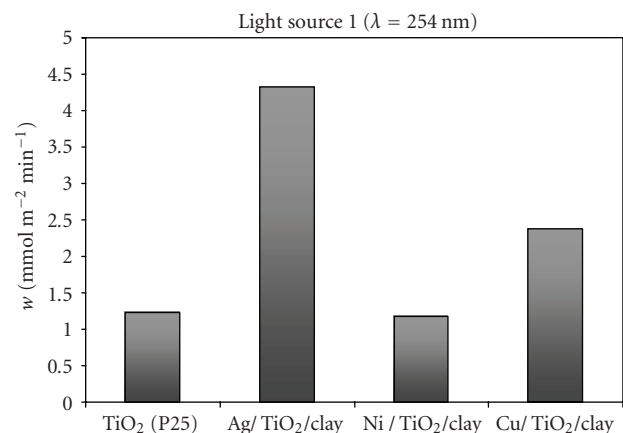
FIGURE 5: Ethanol concentration changes under (a) visible irradiation (light source 2), (b) kinetic curves of acetaldehyde, and (c) CO₂ formation.

the exchange of Ag(I) ions, the intensity of this reflection is lower and $d_{001} = 1.108$ nm because the layered structure will be partially disoriented. However, in the case of Cu(II)- and Ni(II)-ions modified montmorillonite samples, the basal distance is 1.336 nm and 1.445 nm, respectively (Figure 1(a)); that means the nickel and copper ions can be incorporated between the silicate layers, and the two valent cations can close the layers together producing well-oriented lamel-

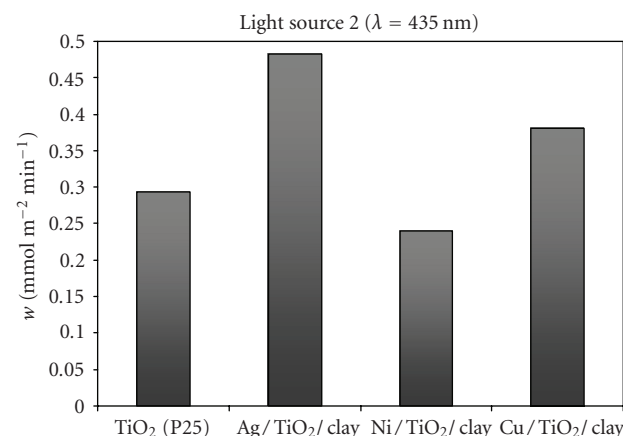
lar structures. After mixing these modified transition metal montmorillonites with TiO₂ powder, the intensity of the clay reflections will be very small, and the interlayer distance will increase to $d_{001} = 1.651$ nm (Ag/TiO₂/clay), $d_{001} = 1.453$ nm (Ni/TiO₂/clay), and $d_{001} = 1.367$ nm (Cu/TiO₂/clay), showing the possibility of the partial incorporation of any TiO₂ nanoparticles between the lamellae (Figure 1(b)). The formation of this suggested structures is presented in Figure 2.

TABLE 2: Photocatalytical characterization of the TiO₂ (P25) and the transition metal nanocomposite samples.

	“Light source 1” ($\lambda = 254$ nm)			“Light source 2” ($\lambda = 435$ nm)		
	Δc_{EtOH} (mmol dm ⁻³) 10 min	k (*10 ⁻⁴ s ⁻¹)	efficiency %	Δc_{EtOH} (mmol dm ⁻³) 10 min	k (*10 ⁻⁴ s ⁻¹)	efficiency %
TiO ₂ (P25)	0.072	6.58	100	0.017	1.43	100
Ag/ TiO ₂ /clay	0.211	34.94	293	0.032	2.31	188
Ni/ TiO ₂ /clay	0.076	6.35	105	0.015	1.22	88
Cu/ TiO ₂ /clay	0.140	13.96	194	0.027	1.88	159



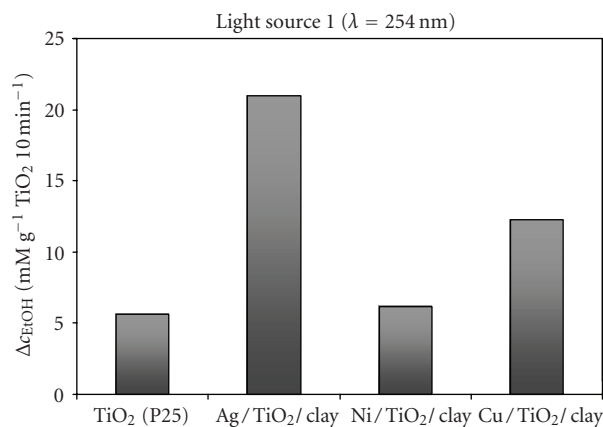
(a)



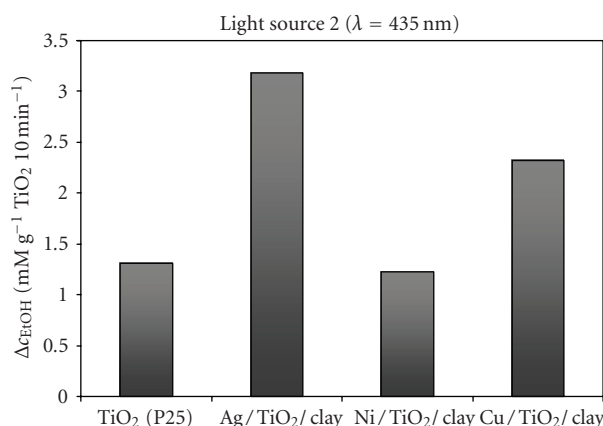
(b)

FIGURE 6: Amount of degraded ethanol in unit time (1 minute), normalized to a catalyst film surface of 1 m²(w).

The photocatalytic efficiency of montmorillonite/ TiO₂ composites was tested in the degradation of ethanol vapor at 70% relative humidity. The reference catalyst was pure Degussa P25 TiO₂. The degradations were also repeated without catalyst with both light sources; it was found that ethanol concentration did not decrease in either case, indicating that self-photolysis does not take place in the vapor studied. The decrease in ethanol concentration and the formation of the main intermediate acetaldehyde were monitored in the course of the measurements (Figures 4(a), 4(b) and 5(a),



(a)



(b)

FIGURE 7: Decreasing of the ethanol concentrations is normalized to 1 g of TiO₂ in unit time (10 minutes).

5(b)). The kinetics of gaseous CO₂ formation was also studied (Figures 4(c), 5(c)). The results of the degradations are summarized in Table 2. In order to characterize catalysts, we introduced the parameter “ w ,” which means the amount of ethanol destroyed by irradiation with the given light source in unit time in a reactor volume of 1 dm³, normalized to a catalyst film surface of 1 m² (Figure 6). The parameter w is calculated by the following equation:

$$w = \frac{\text{amount of degraded EtOH (mmol/dm}^3\text{)}}{\text{time (min)} * \text{surface (m}^2\text{)}}. \quad (1)$$

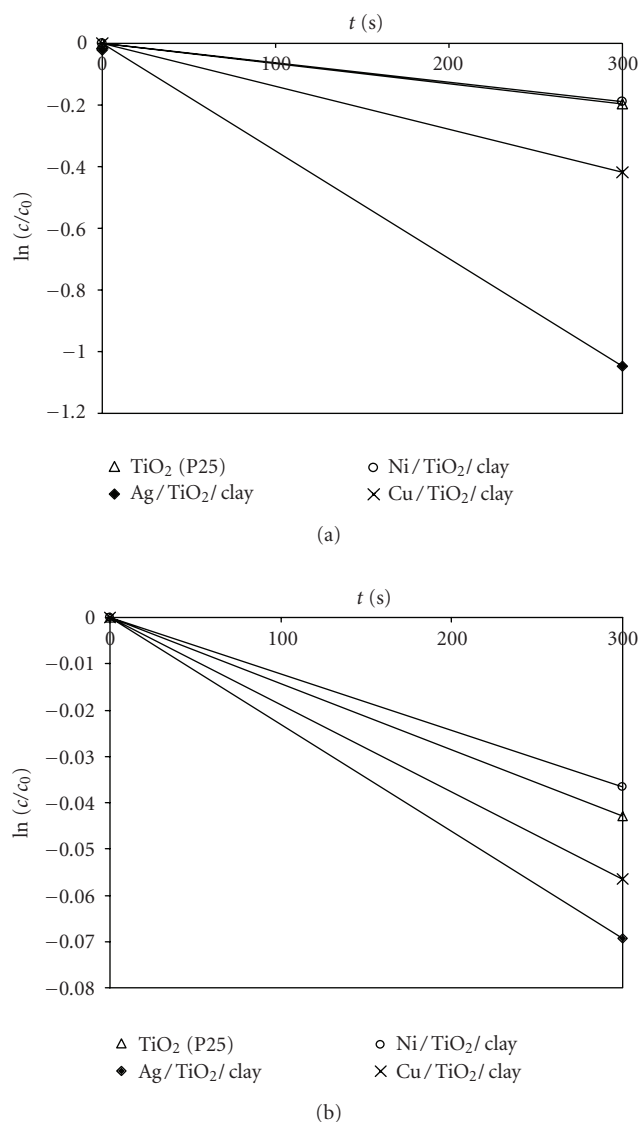


FIGURE 8: Determination of rate constants (k) with $\ln(c/c_0)$ versus t (sec) function by using (a) "light source 1" and (b) "light source 2" lamps.

The measured Δc_{EtOH} values are normalized to 1 g of TiO_2 catalyst and summarized in Figure 7. Table 2 also includes the rate constants (k) calculated from the slopes of the first-order kinetic functions $\ln(c/c_0)$ versus time. The constants unambiguously indicate that the reactions studied follow first-order kinetics (Figures 8(a), 8(b)).

All in all, it can be established that, in the case of each catalyst, ethanol is destroyed much more efficiently by irradiation with the light source rich in UV-C ($\lambda = 254$ nm) than in visible light. The reason for this is well known from the literature: the band gap energy of TiO_2 is $E_g = 3.2$ eV ($\lambda_g = 387$ nm), allowing excitation by light source 1 [27–30]. In the course of photooxidation by both light sources, samples containing silver or copper exhibit higher rates than does the reference TiO_2 sample. The composite containing nickel ions degrades ethanol at a higher rate only in the light of the

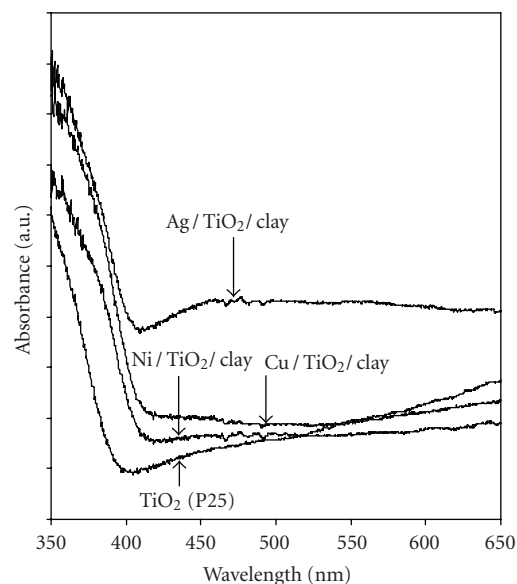


FIGURE 9: Diffuse reflectance UV-Vis spectra of exchanged Na-montmorillonite/ TiO_2 composites.

source rich in UV-C, whereas its efficiency in visible light is identical with that of the reference sample, P25 TiO_2 . Efficiencies (Table 2) are calculated from changes in concentration during a 10-minute irradiation time; ethanol degradation effected by the reference sample Degussa P25 TiO_2 is taken as 100%. The activity of the silver-containing TiO_2/clay composite during irradiation with light source 1 is threefold, and that of the copper-containing composite is twofold over P25 TiO_2 . This extraordinary effect is attributed, on the one hand, to excellent adsorption of ethanol by the layer silicate, allowing fast sorption of ethanol to the TiO_2 surface via diffusion [18]. On the other hand, the doping silver and copper, presumably present in the system in the form of silver and copper oxide nanoparticles, respectively [29, 30], significantly decrease the rate of electron-hole recombination on the TiO_2 surface, increasing catalytic activity. This outstandingly high activity, however, is somewhat decreased in visible light (light source 2), but even in this case, silver and copper degrade ethanol at rates nearly 1.5-fold faster than does P25 TiO_2 . We assume that the reason for this is an increased photon absorbance in the visible wavelength range ($\lambda = 400$ – 700 nm) on the composites prepared by us, as demonstrated by the absorbance spectra shown in Figure 9. The spectrum of $\text{Ni/TiO}_2/\text{clay}$ and Cu -loaded TiO_2/clay displays similar absorbance at wavelengths shorter than 410 nm, while $\text{Cu/TiO}_2/\text{clay}$ absorbs more photons whose wavelengths are larger than 410 nm, resulting in the color of light green. The sample of $\text{Ag/TiO}_2/\text{clay}$ possesses an additional broadened absorption peak at about 450 nm in the visible region, that indicates the brown color of the deposited silver can improve the light absorption of $\text{Ag/TiO}_2/\text{clay}$ and increase its photocatalytic activity. In other words, the efficiency of degradation in visible light can be explained by the excellent adsorption properties of the layer silicate and the red shift of photon absorbance at higher wavelengths.

4. CONCLUSIONS

Photocatalytic utilization of titanium dioxide and its composites with clay mineral support was studied in a vapor phase oxidation reaction. Since results on direct doping of TiO₂ with transient metals reported in the literature did not show an unambiguous increase in efficiency, we used 20% montmorillonite support exchanged with silver, copper, or nickel ions and mixed/ground with P25 TiO₂ in powder form. The amounts of metal normalized to the total mass of the catalyst were Ag: 2.16%, Cu: 0.64%, and Ni: 0.59%. The composite obtained was used for the preparation of films on the surface of the glass reactor, where photooxidation was carried out. The rate of photooxidation by irradiation with the light source rich in UV-C ($\lambda = 254$ nm) increased significantly as a result of the introduction of silver or copper included in the layer silicate, and the rate of the photooxidation process in visible light was also higher than that measured in the presence of the reference sample P25 TiO₂.

REFERENCES

- [1] P. Pichat, J. Disdier, C. Hoang-Van, D. Mas, G. Goutailler, and C. Gaysse, "Purification/deodorization of indoor air and gaseous effluents by TiO₂ photocatalysis," *Catalysis Today*, vol. 63, no. 2–4, pp. 363–369, 2000.
- [2] L. Zhang and J. C. Yu, "A simple approach to reactivate silver-coated titanium dioxide photocatalyst," *Catalysis Communications*, vol. 6, no. 10, pp. 684–687, 2005.
- [3] Z. Guo-Min, C. Zhen-Xing, X. Min, and Q. Xian-Qing, "Study on the gas-phase photolytic and photocatalytic oxidation of trichloroethylene," *Journal of Photochemistry and Photobiology A: Chemistry*, vol. 161, no. 1, pp. 51–56, 2003.
- [4] S. B. Kim, H. T. Hwang, and S. C. Hong, "Photocatalytic degradation of volatile organic compounds at the gas-solid interface of a TiO₂ photocatalyst," *Chemosphere*, vol. 48, no. 4, pp. 437–444, 2002.
- [5] G. Marci, M. Addamo, V. Augugliaro, et al., "Photocatalytic oxidation of toluene on irradiated TiO₂: comparison of degradation performance in humidified air, in water and in water containing a zwitterionic surfactant," *Journal of Photochemistry and Photobiology A: Chemistry*, vol. 160, no. 1–2, pp. 105–114, 2003.
- [6] Z. Pengyi, L. Fuyan, Y. Gang, C. Qing, and Z. Wanpeng, "A comparative study on decomposition of gaseous toluene by O₃/UV, TiO₂/UV and O₃/TiO₂/UV," *Journal of Photochemistry and Photobiology A: Chemistry*, vol. 156, no. 1–3, pp. 189–194, 2003.
- [7] T. Sano, N. Negishi, K. Takeuchi, and S. Matsuzawa, "Degradation of toluene and acetaldehyde with Pt-loaded TiO₂ catalyst and parabolic trough concentrator," *Solar Energy*, vol. 77, no. 5, pp. 543–552, 2004.
- [8] G.-M. Zuo, Z.-X. Cheng, H. Chen, G.-W. Li, and T. Miao, "Study on photocatalytic degradation of several volatile organic compounds," *Journal of Hazardous Materials*, vol. 128, no. 2–3, pp. 158–163, 2006.
- [9] A. Di Paola, M. Addamo, M. Bellardita, E. Cazzanelli, and L. Palmisano, "Preparation of photocatalytic brookite thin films," *Thin Solid Films*, vol. 515, no. 7–8, pp. 3527–3529, 2007.
- [10] M. Addamo, M. Bellardita, A. Di Paola, and L. Palmisano, "Preparation and photoactivity of nanostructured anatase, rutile and brookite TiO₂ thin films," *Chemical Communications*, no. 47, pp. 4943–4945, 2006.
- [11] D. Dvoranová, V. Brezová, M. Mazúr, and M. A. Malati, "Investigations of metal-doped titanium dioxide photocatalysts," *Applied Catalysis B: Environmental*, vol. 37, no. 2, pp. 91–105, 2002.
- [12] K. Chiang, R. Amal, and T. Tran, "Photocatalytic degradation of cyanide using titanium dioxide modified with copper oxide," *Advances in Environmental Research*, vol. 6, no. 4, pp. 471–485, 2002.
- [13] Slamet, H. W. Nasution, E. Purnama, S. Kosela, and J. Gunlazuardi, "Photocatalytic reduction of CO₂ on copper-doped Titania catalysts prepared by improved-impregnation method," *Catalysis Communications*, vol. 6, no. 5, pp. 313–319, 2005.
- [14] K. Mogyorósi, I. Dékány, and J. H. Fendler, "Preparation and characterization of clay mineral intercalated titanium dioxide nanoparticles," *Langmuir*, vol. 19, no. 7, pp. 2938–2946, 2003.
- [15] T. Pernyeszi and I. Dékány, "Photocatalytic degradation of hydrocarbons by bentonite and TiO₂ in aqueous suspensions containing surfactants," *Colloids and Surfaces A: Physicochemical and Engineering Aspects*, vol. 230, no. 1–3, pp. 191–199, 2004.
- [16] C. Ooka, H. Yoshida, K. Suzuki, and T. Hattori, "Effect of surface hydrophobicity of TiO₂-pillared clay on adsorption and photocatalysis of gaseous molecules in air," *Applied Catalysis A: General*, vol. 260, no. 1, pp. 47–53, 2004.
- [17] R. Kun, M. Szekeres, and I. Dékány, "Photooxidation of dichloroacetic acid controlled by pH-stat technique using TiO₂/layer silicate nanocomposites," *Applied Catalysis B: Environmental*, vol. 68, no. 1–2, pp. 49–58, 2006.
- [18] J. Liu, X. Li, S. Zuo, and Y. Yu, "Preparation and photocatalytic activity of silver and TiO₂ nanoparticles/montmorillonite composites," *Applied Clay Science*, vol. 37, no. 3–4, pp. 275–280, 2007.
- [19] R. Kun, K. Mogyorósi, and I. Dékány, "Synthesis and structural and photocatalytic properties of TiO₂/montmorillonite nanocomposites," *Applied Clay Science*, vol. 32, no. 1–2, pp. 99–110, 2006.
- [20] J. Araña, J. M. Doña-Rodríguez, O. González-Díaz, et al., "Gas-phase ethanol photocatalytic degradation study with TiO₂ doped with Fe, Pd and Cu," *Journal of Molecular Catalysis A: Chemical*, vol. 215, no. 1–2, pp. 153–160, 2004.
- [21] D. S. Muggli, J. T. McCue, and J. L. Falconer, "Mechanism of the photocatalytic oxidation of ethanol on TiO₂," *Journal of Catalysis*, vol. 173, no. 2, pp. 470–483, 1998.
- [22] E. Piera, J. A. Ayllón, X. Doménech, and J. Peral, "TiO₂ deactivation during gas-phase photocatalytic oxidation of ethanol," *Catalysis Today*, vol. 76, no. 2–4, pp. 259–270, 2002.
- [23] M. R. Nimlos, E. J. Wolfrum, M. L. Brewer, J. A. Fennell, and G. Bintner, "Gas-phase heterogeneous photocatalytic oxidation of ethanol: pathways and kinetic modelling," *Environmental Science and Technology*, vol. 30, no. 10, pp. 3102–3110, 1996.
- [24] M. L. Sauer and D. F. Ollis, "Catalyst deactivation in gas-solid photocatalysis," *Journal of Catalysis*, vol. 163, no. 1, pp. 215–217, 1996.
- [25] M. L. Sauer and D. F. Ollis, "Photocatalyzed oxidation of ethanol and acetaldehyde in humidified air," *Journal of Catalysis*, vol. 158, no. 2, pp. 570–582, 1996.

- [26] L. Kőrösi, A. Oszkó, G. Galbács, A. Richardt, V. Zöllmer, and I. Dékány, "Structural properties and photocatalytic behaviour of phosphate-modified nanocrystalline titania films," *Applied Catalysis B: Environmental*, vol. 77, no. 1-2, pp. 175–183, 2007.
- [27] H. Li, Z. Bian, J. Zhu, Y. Huo, H. Li, and Y. Lu, "Mesoporous Au/TiO₂ nanocomposites with enhanced photocatalytic activity," *Journal of the American Chemical Society*, vol. 129, no. 15, pp. 4538–4539, 2007.
- [28] C. Burda, Y. Lou, X. Chen, A. C. S. Samia, J. Stout, and J. L. Gole, "Enhanced nitrogen doping in TiO₂ nanoparticles," *Nano Letters*, vol. 3, no. 8, pp. 1049–1051, 2003.
- [29] T. Morikawa, Y. Irokawa, and T. Ohwaki, "Enhanced photocatalytic activity of TiO_{2-x}N_x loaded with copper ions under visible light irradiation," *Applied Catalysis A: General*, vol. 314, no. 1, pp. 123–127, 2006.
- [30] I. Dékány, L. Turi, and Z. Király, "CdS, TiO₂ and Pd⁰ nanoparticles growing in the interlamellar space of montmorillonite in binary liquids," *Applied Clay Science*, vol. 15, no. 1-2, pp. 221–239, 1999.